Friction
https://doi.org/10.1007/s40544-022-0612-y
ISSN 2223-7690
CN 10-1237/TH
RESEARCH ARTICLE

Fingerprint inspired advanced end-effector and its applications

Sung Ho LEE[1], **Hyo Sung KIM**[2], **Han Jun PARK**[2], **Moon Kyu KWAK**[2,*]

[1] *Department of Electrical Engineering and Computer Science, University of Michigan, Ann Arbor 48109, USA*

[2] *Department of Mechanical Engineering, Kyungpook National University, Daegu 41566, Republic of Korea*

Received: 21 December 2021 / Revised: 20 January 2022 / Accepted: 28 February 2022

Abstract: The human fingertip consists of a fingerprint with many micro-grating structures. The main roles of the fingerprint could be divided into two purposes, namely, the enhancement of the frictional force and the effective transmittance of the biosignal. In this study, we present the fingerprint-inspired end-effector that has not only admirable frictional force but also electric conductivity. The end-effector is composed of fluorocarbon rubber, one of the famous materials to achieve high frictional force and robustness. Through various experiments, the novel performance of micro structured fluorocarbon rubber end-effector (MSFE) is characterized by comparing with a macroscale patterned sample (MPS), which has been already used in real industrial fields. Experimental results are analyzed theoretically. Furthermore, as feasible applications, we suggest two applications based on the role of the fingerprint. One is the conductive astronaut glove with high frictional force, and the other one is a non-slip pad for the next-generation glass transfer systems. Through these experiments, we successfully observe the enhanced system performance and confirm the possibility of using the MSFE as feasible applications. We believe that the MSFE could be a useful and powerful alternative as an end-effector, not only in the aerospace industry but also in display manufacturing processes.

Keywords: fingerprint; end-effector; fluorocarbon rubber (FKM); glass transfer system; spacesuit

1 Introduction

Most living creatures, even humans, have evolved to survive with a new personal surviving method; they have also attempted to effectively adapt to the surrounding environment by optimizing the energy consumption mechanisms [1–3]. To apply their effective living methods in our life, many studies have been actively carried out from macro to micro perspective view in terms of biomimetics [4–21]. As a representative example of this evolution, the end of the human's finger or toe has unique prints that consist of macro/micro grating structures with a width of ~200 μm and a period of ~500 μm. The fingerprint formation is initiated from the womb and is grown large during childhood. The fingerprint shape is unique to each individual, even for identical twins, and it does not change [22–23]. Therefore, the uniqueness of fingerprint has been widely used in individual detection, such as in criminal investigation or electric security [24–26]. Generally, the instinct role of the fingerprint could be largely divided into two purposes: One is a precise grasping of object, and the other is an enhancement of the tactile sensitivity. Frictional force and transmittance of biosignal increased because the macro/microstructures of fingerprint allow the expansion of a contact area with surfaces. Therefore, a human can grip the object stably and detect the fine object effectively [27–29].

Fluorocarbon rubber, a type of thermoset elastomer, has been an actively-used material in various industrial fields. This material is composed of a strong combination of fluorine–carbon chemical binding and has many advantages, such as admirable frictional force,

*Corresponding author: Moon Kyu KWAK, E-mail: mkkwak@knu.ac.kr

high thermal and chemical resistance, and low outgassing in extremely high vacuum condition [30–36]. Considering its various advantages, the fluorocarbon rubber has been actively used as a non-slip pad and as an end-effector for glass transfer systems. However, the enhancement of an advanced end-effector along with the development of a new display product with larger and heavier display glass has been required [37]. To improve the performance of a conventional end-effector, many novel studies that use a functional surface composed of micro/nano structures have been presented [8, 38–43]. Although various functional surfaces with complex shape of micro/nano structures were achieved, the fabrication of the functional surface that consists of the micro structures using fluorocarbon rubber has been limited because this process requires high pressure and temperature. Typically, to form the micro structure onto surface, a micro structured mold or stamp is required. Therefore, micro structures consist of polymers with a substrate, such as poly ethylene terephthlate (PET) film, or are directly formed on the silicon wafer [44–47]. Therefore, if these microstructured surfaces are used as stamps in the fabrication process of fluorocarbon rubber, and then the thermal degradation of polymer or the failure of the silicon wafer could occur because of high pressure and temperature. Therefore, a new fabrication method is required to fabricate samples that are composed of the micro structured flulorocarbon rubber.

Herein, we introduce a micro structured fluorocarbon rubber end-effector (MSFE) inspired by the role of fingerprint and a new fabrication method for the fluorocarbon rubber. To form the microstructure on the fluorocarbon surface, the thin poly(dimethylsiloxane) (PDMS) sheet was used as a flexible mold, and the MSFE exhibited admirable performance, such as high frictional force and electric conductivity. The comparison of various experiments with a macroscale patterned sample (MPS), which has been used in real industrial fields, shows the excellence of the MSFE. The frictional force of MSFE was measured as ~22.3 N, which is a value that is up to 4.5 times higher than the frictional force of MPS. Moreover, to confirm the possibility of using the MSFE in real industrial fields, additional experiments, such as pull-off strength, 100,000 repeat tests, and thermogravimetric analysis (TGA) test, were implemented. Lastly, the experiments introduced the MSFE-applied astronaut glove and the six degrees of freedom (6-DOF) robot arm as feasible applications. Through these experiments, the novel performance of MSFE was verified, and the new fabrication method for the microstructured fluorocarbon rubber was introduced. We believe that the MSFE and the new fabrication method could be utilized in various fields, such as in the next-generation glass transfer systems and astronaut gloves.

2 Experimental

2.1 Fabrication of MSFE

To form the microstructure on the fluorocarbon rubber surface, a thin PDMS sheet with microstructures was used as the flexible mold. After placing an appropriate amount of fluorocarbon rubber material (DC7360CX, Wooshin Chemtech, Republic of Korea) on the PDMS mold, heat energy (180 °C) and pressure (1,600 kPa) were applied for 450 s. After cooling for 2 h, the MSFE was separated from the PDMS mold. Also, the MPS was gladly provided by a non-slip pad manufacturer (NSP-bs12, BSTECH, Republic of Korea).

2.2 Fabrication of flexible mold

To fabricate the MSFE, a thin PDMS sheet was prepared as the flexible mold. The PDMS mixture was prepared with a 10:1 weight ratio of the elastomer base and the curing agent (Sylgard 184 kit, Dow Corning Corp., USA). Degassed PDMS mixture was poured onto the master mold with micro-prism arrays and was uniformly spread to create thin PDMS sheets. The cured-thin PDMS sheet was carefully separated from the master mold after 2 h in a 70 °C oven. Finally, the thin PDMS stamp for the flexible mold was prepared.

2.3 Characteristics of surface topology

To observe the surface topology of the sample, various experimental instruments such as the optical microscope (LV150L, Nikon, Japan), scanning electron microscope (SEM; S-4800, Hitachi, Japan), and atomic force microscope (AFM; NX20, Park Systems, Republic of Korea), were utilized. Especially, before the SEM measurement, a thin metal layer (Pt < 5 nm) was

formed on the surface of the sample to prevent the electron charging at high voltages (10–25 kV).

2.4 Measurement of the frictional force and pull-off strength

A precise digital force gauge and custom-built equipment were used to measure the frictional force and the pull-off strength with the glass substrate. Frictional force was measured several times after that a preload of 500 g was located on the sample surface. Similar to our previous works, the pull-off strength was measured by a custom-built equipment [40, 43].

2.5 Material properties of MSFE

The electric conductivity of MSFE was characterized by using a surface resistance meter (SRM 200, Wolfgang Warmbier, Germany) at room temperature. Several points were randomly measured for each sample. The thermal stability of the MSFE was characterized by using an auto-thermogravimetric analyzer (Q500 model, Waters Corp., USA) at wide temperature range. The temperature was increased from room temperature to 400 °C with an increasing rate of 10 °C·min^{-1} in air conditions, and the residual weight according to the increasing temperature was exhibited compared with the original weight of the sample. Also, the chemical component was characterized by using the Fourier transform infrared (FTIR) spectroscope (Frontier, Perkinelmer Corp., USA).

3 Results and discussion

3.1 Fabrication and design

An experimental sample having the electrical signal transmission and high frictional force inspired by the two main roles of fingerprint was designed, and a fluorocarbon rubber was used as the experimental material (Fig. 1(a)). As shown in Fig. 1(b), the fluorocarbon rubber, which consists of a strong bond of carbon and fluoride compounds, is a well-known material with various advantages of being usable under harsh conditions (e.g., during high temperature and vacuum conditions) and for having admirable frictional force. Although the advantages are numerous, the fluorocarbon rubber sample has a critical problem that needs to be improved to fabricate a microstructured

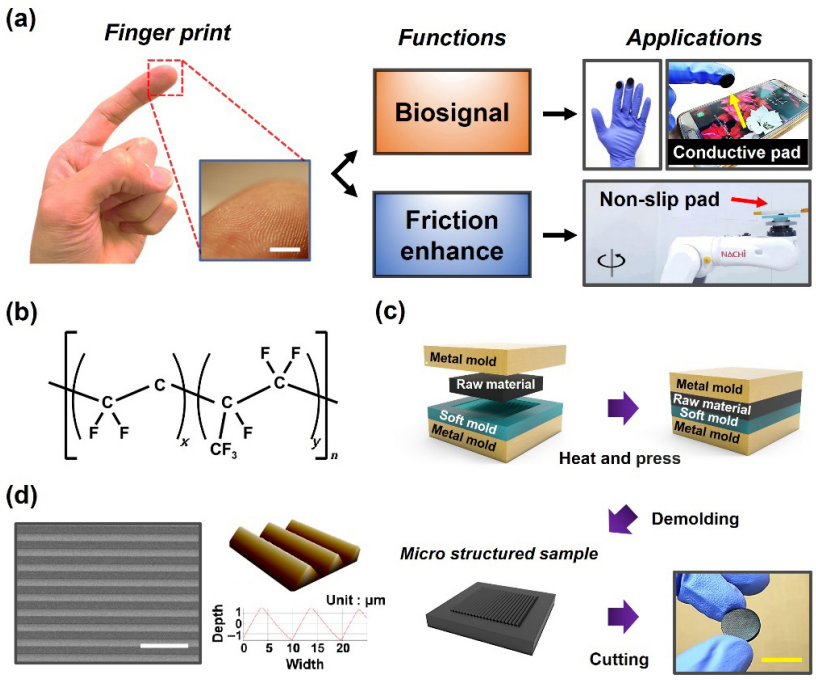

Fig. 1 Introduction of the MSFE. (a) Photograph of the human fingerprint and applications of the MSFE based on the performance of fingerprint. (b) Image of the chemical structure for the fluorocarbon rubber. (c) Illustration of fabrication method for the micro structured sample composed of the fluorocarbon rubber. Scale bar (yellow) is 15 mm. (d) SEM and AFM images of the MSFE surface with micro-scale prism shape of 10 μm width and 4 μm height. Scale bar (white) is 30 μm.

fluorocarbon rubber sample. Most of the microstructures are formed on the silicon wafer. Moreover, the use of silicon mastermold directly to the fabrication of fluorocarbon rubber has been limited because high pressure and temperature are required. If the silicon mastermold with the microstructures is used directly in the fluorocarbon rubber fabrication process, and then the mastermold could be easily damaged. Therefore, the fabrication of fluorocarbon rubber sample with microstructures has been limited so far. To overcome this problem, a new fabrication strategy for the microstructured fluorocarbon rubber sample was developed using a microstructured flexible mold. PDMS, which is a kind of thermoset polymer that is mainly used in soft lithography, has been used as a flexible mold material (Fig. S1 in the Electronic Supplementary Material (ESM)). The PDMS has various advantages, with a high resolution to replicate micro/nano structures, and the maximum operational temperature range of PDMS is ~200 °C [48–49]. Therefore, the PDMS could be used as the flexible mold in this fabrication process carried out at 180 °C. As shown in Fig. 1(c), after placing a uniform and thin PDMS mold with microstructures between the metal molds, an appropriate amount of fluorocarbon rubber was placed on the PDMS mold. Moreover, to use the PDMS in this fabrication process, the relationship of the surface energy between PDMS and fluorocarbon rubber is important and has shown a low value to easily demold the fluorocarbon rubber from the PDMS mold after finishing the fabrication process. The demolding strength of the fluorocarbon rubber from PDMS is predictable, and this energy relationship could be expressed by the "work of adhesion (W)", which is the energy required for the detachment between two contact surfaces i and j and can be represented as follows [50–51]:

$$W_{ij} = \frac{4\gamma_i^{\mathrm{d}}\gamma_j^{\mathrm{d}}}{\gamma_j^{\mathrm{d}} + \gamma_j^{\mathrm{d}}} + \frac{4\gamma_i^{\mathrm{p}}\gamma_i^{\mathrm{p}}}{\gamma_i^{\mathrm{p}} + \gamma_i^{\mathrm{p}}} \quad (1)$$

where γ is the surface energy; and the superscripts d and p are the dispersion and polar terms, respectively. When the work of adhesion is calculated using the values in Table 1 and Eq. (1), the work of adhesion between the PDMS and the fluorocarbon rubber ($W_{\mathrm{PDMS/fluorocarbon\ rubber}}$) was calculated as ~8.9 mJ·m^{-2}, which is quite a low value (Calculation section 1 in the ESM). This calculation result indicates that the fluorocarbon rubber sample can be demolded much easily from the PDMS mold, and the PDMS, as a flexible mold, is a suitable material for this fabrication process. To observe the surface of the fabricated MSFE, surface topology was characterized by using the SEM and AFM (Fig. 1(d)), and the microstructure with a prism shape of 10 μm width and 4 μm height was used as a stamp and was well-formed on the MSFE surface. Also, to present the electric conductivity property for the biosignal transmission, a carbon black was added as a conductive material in the fluorocarbon rubber. The surface resistance of the MSFE was measured as 5 × 10^4 Ω, and the electric conductivity of MSFE was successfully observed (Fig. S2 in the ESM) [52–54].

Table 1 Surface energy of various materials.

Material	γ^{d} (mJ·m^{-2})	γ^{p} (mJ·m^{-2})
Glass	28.2	35.6
PDMS	21.7	1.1
Fluorocarbon rubber	0.8	12.7

3.2 Performance of the MSFE

To evaluate the performance of the MSFE, various characteristic tests were conducted, and the results were detailed in Fig. 2. The key point of MSFE is a high frictional force. The MSFE exhibited remarkably high frictional force with the glass substrate, and it could be largely analyzed from two perspectives: One is an inherent material property, and the other is the structural mechanics.

The first reason of showing the high frictional force with the glass substrate was the inherent material property of the fluorocarbon rubber and could be analyzed by using the work of adhesion. To slip, the surface between the fluorocarbon rubber and the glass substrate must be detached. From the surface energy in Table 1, the work of adhesion between the fluorocarbon rubber and the glass substrate ($W_{\mathrm{glass/fluorocarbon\ rubber}}$) was calculated and obtained a remarkably high value of 40 mJ·m^{-2}. That is, high amounts of energy are required to detach the MSFE

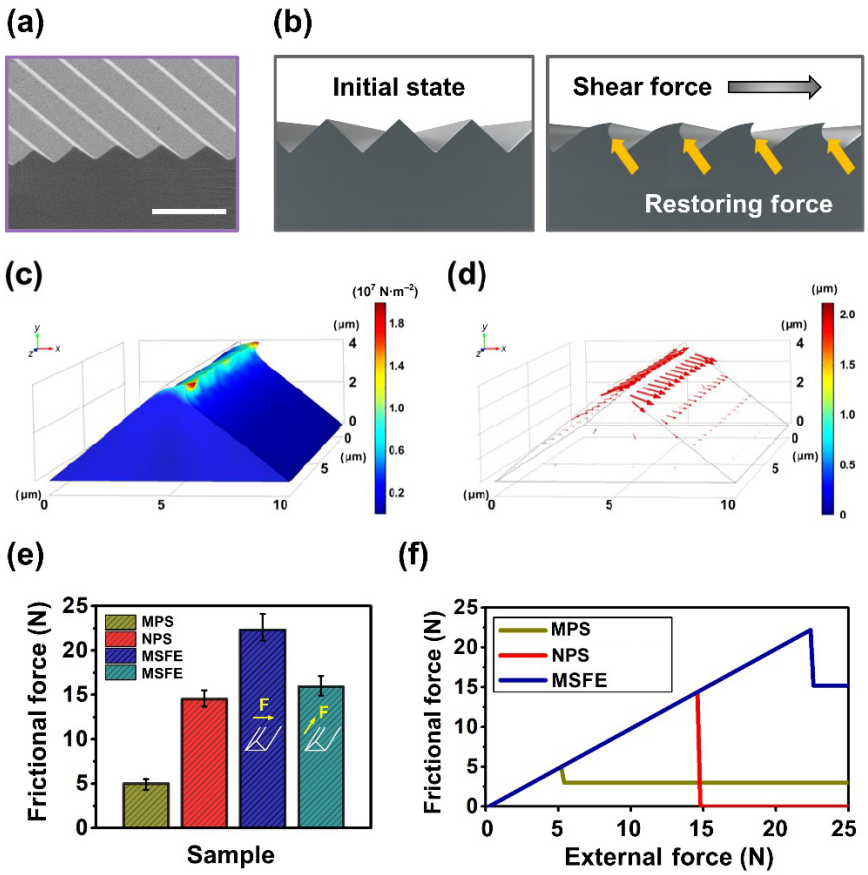

Fig. 2 (a) SEM image of the cross-section of the MSFE. Scale bar is 30 μm. (b) Illustration of the deformation of microstructures depending on the external force. (c) Simulation result of the stress of the unit micro-scale prism. (d) Simulation result of the deformation of unit micro-scale prism. (e) Measurement result of the frictional force with respect to various samples; MPS, NPS, MSFE (in the horizontal/vertical direction with respect to the micro-prism). (f) Measurement result of the dynamic friction.

from the glass substrate. Therefore, the MSFE could exhibit the high frictional force with the glass substrate.

Additionally, the second factor for enhancing the frictional force was the microstructures on the MSFE surface, and it was an important parameter for this study. As shown in Fig. 2(a), microprism structures were formed on the MSFE surface. When an external force is applied, the structural deformation of the microstructure occurred through the external force, and this structural deformation at the elastic region makes a high restoring force (Fig. 2(b)). At this time, the behavior of the unit microprism could be analyzed as a cantilever beam, and the external force (F) could be expressed as follows [55]:

$$F = \frac{3EI}{L^3} \cdot \delta \tag{2}$$

where I is the moment of inertia of the cross-sectional area; L is the length of the cantilever beam; and E and δ are the Young's modulus (8.2 MPa) and deformation, respectively. The microstructures on the MSFE surface were deformed by external force. Thus, the external force was converted into the restoring force in the elastic region. Therefore, the MSFE could exhibit a tremendous frictional force since the restoring force by the microstructures was added to the inherent frictional force of the fluorocarbon rubber. In addition, stress and deformation of the microstructure on the MSFE were simulated on the basis of the above parameters (Figs. 2(c) and 2(d)). The top of the unit microstructure was bent in the same direction as the external force, and the maximum pressure and the deformation were shown as ~20 MPa and ~2 μm, respectively.

To observe the frictional force of the MSFE, the

friction test was conducted by comparing it with three samples, namely, MPS, non-patterned sample (NPS), and MSFE. The MPS with an embossed surface (height = 70 μm, period = 500 μm) has been used as a non-slip pad of the real glass transfer systems in industrial fields (Fig. S3 in the ESM). In addition, the frictional force of NPS was measured to compare the effectiveness of the microstructures on the MSFE surface. The frictional force of each sample was characterized with a preload of 500 g, and the MSFE inspired by the fingerprint was revealed to exhibit significantly enhanced frictional force compared with the other samples.

The frictional force of the MPS and NPS was measured as 5.00 and 14.51 N, respectively, whereas the MSFE was exhibited a remarkably high frictional force of 22.32 N. This result was up to ~4.5 times improved value compared with the other samples. Furthermore, as shown in Fig. 2(e), the frictional force of the MSFE was measured much higher than that of the NPS. This result could be a strong evidence to prove the effectiveness of the microstructure on the MSFE surface and was the key feature of MSFE. The frictional force was highly increased in the MSFE case because the restoring energy of the microstructures was added on the inherent material friction (Fig. 2(b)). In addition, the effectiveness of the microstructure was shown additionally in Fig. 2(e). The micro-prism structure of the MSFE was arrayed in one direction, the frictional force was measured differently depending on the frictional direction, and the directionality was shown in Fig. 2(e). When the external force was applied in a direction perpendicular to the micro-prism array (Fig. 2(e), blue bar), the frictional force was measured as 22.34 N; and when the external force was applied in a direction parallel to the micro-prism array (Fig. 2(e), green bar), the frictional force was measured as 15.23 N. It was 7.09 N lower than that of the perpendicular case (Fig. S4 and Calculation section 2 in the ESM). As is previously shown in Fig. 2(b), this result could be another piece of evidence for the enhancement of the frictional force due to the microstructures. When the external force is applied in a parallel direction with the micro-prism array, the moment of inertia of the microstructure is much higher than that in the perpendicular case. As a result, the deformation of microstructures due to the external force was decreased greatly. Therefore, the effect of frictional enhancement by the deformation of micro-structures was nearly neglectable compared with the perpendicular case. As a result, the frictional force in a parallel direction with the micro-prism array was almost similar to the NPS case, and this was a quite reasonable result.

Meanwhile, the human fingerprint is composed of many grating structures, indicating that new frictional force is generated continuously even if a slip occurred. This performance of the fingerprint could be an additional advantage for the stable usage of the MSFE, and it could also be applied to the MSFE inspired by the fingerprint. To observe this performance, dynamic friction was measured (Fig. 2(f)). In the NPS case (red line), it was shown as a high frictional force in the static friction range, however, after slip occurred, no dynamic friction was measured, and the glass substrate strongly escaped from the NPS surface because the glass substrate was detached immediately. It could be a significant disadvantage to apply to real applications because unexpected slips could frequently occur in real situations. The MPS and MSFE exhibited admirable dynamic friction. Especially, in the MSFE case (blue line), it not only shows the admirable static friction (~22.2 N) but also the high dynamic friction (~15.2 N). As shown in Fig. 3, considering that the MSFE consists of numerous microstructures, a new

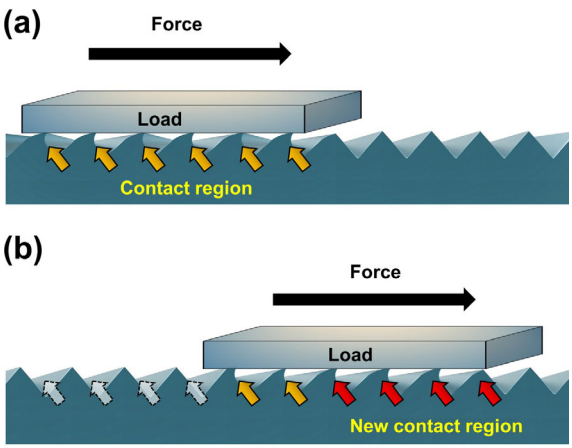

Fig. 3 Illustration of the principle of the dynamic friction-enhancement of the MSFE. (a) Initial status before the slip. The orange-coloured arrows indicate the initial contact region with the MSFE. (b) Schematic of the friction after occurring the slip. The new contact region was generated continuously by the micro structures on the MSFE surface. The red-coloured arrows indicate the new contact region with the MSFE.

contact area between the microstructures and glass substrate was continuously generated because of the microstructures. Thus, the high dynamic friction was exhibited in the MSFE sample, and more stable usage could be allowed.

Through the measurement of the frictional force, the admirable performance of the MSFE was observed. To apply the MSFE as a feasible application in real life, additional characteristic experiments were carried out. Through the various experiments, the frictional force of the MPS was measured to be a relatively low value compared with the other samples. Despite the relatively low frictional force, the reason why the MPS has been used as a non-slip pad in the real glass transfer systems was shown in Fig. 4(a). As the next-generation glass becomes larger and thinner in the display market, a development of the advanced non-slip pad with microstructures having not only a high frictional force but also a low adhesive force has been required. However, forming the microstructure on the fluorocarbon rubber pad surface is difficult. Furthermore, although the fabrication process of the NPS is much easier than the MPS fabrication process, and the NPS shows much higher frictional force than that of the MPS, the NPS could not be used because of a critical limitation in terms of an adhesion issue. If the non-slip pad has the adhesion in the vertical direction when the pad is detached from the glass, then the thin glass substrate could be damaged. Therefore, the low adhesion is an important factor for glass transfer systems, and the pull-off strength was measured by a custom-built equipment (Fig. S5 in the ESM). As shown in Fig. 4(a), the NPS showed a high pull-off strength of up to ~250 kPa, whereas MPS and MSFE exhibited no pull-off strength. Generally, the vertical adhesion is proportional to the contact area on the contact surface, and the pull-off strength (P) could be simply expressed as follows [56–59]:

$$P = \frac{3}{2}\pi RW \tag{3}$$

where R is the radius of the hemisphere in contact, and W is the work of adhesion. In the case of MSFE, the line contact with the glass surface occurred, and the value of R was considered ~0 because the MSFE was composed of the micro-prism array. Therefore, the MSFE could exhibit not only the high frictional force but also no pull-off strength because of the microstructures. Thus, the MSFE could be a suitable application as the non-slip pad for the glass transfer systems without causing any damage to the glass substrate.

Another advantage of the fluorocarbon rubber is its robustness. To use the MSFE in actual industrial fields or in real life, it must maintain excellent performance without deteriorating even after many repetitive usages. To confirm the sustainability of the MSFE, 100,000 cycle repeat tests were implemented by applying a preload of 50 kPa. As shown in Fig. 4(b), the frictional force of the MPS was well-maintained at 4.50 and 4.80 N after 50,000 and 100,000 cycles, respectively. Likewise, in the MSFE case, the high frictional force was measured as 21.52 and 22.13 N after 50,000 and 100,000 cycles, respectively. Both samples showed a similar value compared with the initial frictional force (5.00 and 22.32 N) after the repeat tests, indicating that the MSFE could be used stably without deterioration of performance even after repeated use of 100,000 times.

Furthermore, the fluorocarbon rubber is one of the famous materials that can be used at high temperature and vacuum conditions. To observe the thermal resistance of the MSFE, an experiment for thermal

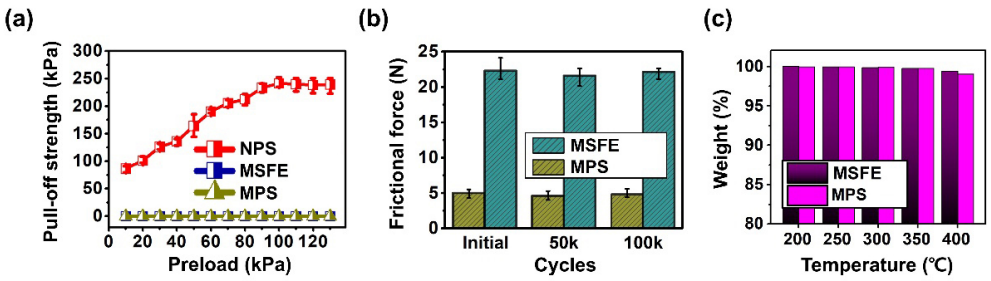

Fig. 4 (a) Measurement result of the pull-off strength with respect to various preloads. (b) Experimental result of the frictional force measurement according to the 100k repeat test. (c) TGA result of the MSFE and the MPS of up to 400 ℃.

stability was carried out by using the TGA to predict the thermal degradation of materials. As shown in Fig. 4(c), the residual weights of the MSFE and the MPS compared with the initial weight at 200 °C were measured as 99.99% and 99.95%, respectively. The residual weights of the MSFE and the MPS at 300 °C were measured as 99.87%, 99.92%, respectively. At 400 °C, despite a quite high temperature, the MSFE and the MPS showed the high residual weights of 99.43% and 99.01%, respectively. These results indicated that the MSFE and the MPS could be used stably and reliably in quite a wide temperature range.

3.3 Applications

Based on various experiments, it turned out that the MSFE could be applied to various fields.

As mentioned before, the fingerprint enhances the efficiency of biosignal transmission and frictional force. So far, through the various experiments, the admirable performance of the MSFE inspired by the fingerprint, such as conductivity, high frictional force, and sustainability, were revealed. In this section, we suggest two experiments as feasible applications of the MSFE based on the role of the fingerprint: One is an astronaut glove with the MSFE, and the other is a frictional force-enhanced non-slip pad for the glass transfer systems.

In space, astronauts must wear a spacesuit to protect themselves from the harsh space environment. The MSFE can be utilized at high temperature and vacuum condition and has conductivity. As the first feasible application, a conductive glove with the MSFE was introduced by assuming the astronaut glove. As shown in Fig. 5(a), the MSFE was attached to the tip of the experimental glove, assuming a situation, in which electrical signals must be transmitted to the outside while wearing a spacesuit. As shown in Fig. 5(b), the electrical signal was well transmitted through the MSFE, and the touch screen of the electronic device could be operated without taking off the gloves. Through this experiment, the possibility of using the MSFE for the astronaut glove was observed, and the glove with the MSFE could improve the research performance and efficiency and user convenience in the daytime space environment by manipulating the external touch screen effectively while increasing the grip power of the outer space suit.

As a second feasible application, an experiment for the glass transfer systems by using the MSFE was conducted. Various novel performances of the MSFE were revealed and compared with the MPS, and the MSFE could be a suitable non-slip pad for the advanced glass transfer systems. As shown in Fig. 5(c), the experiment was implemented with a 6-DOF robot arm.

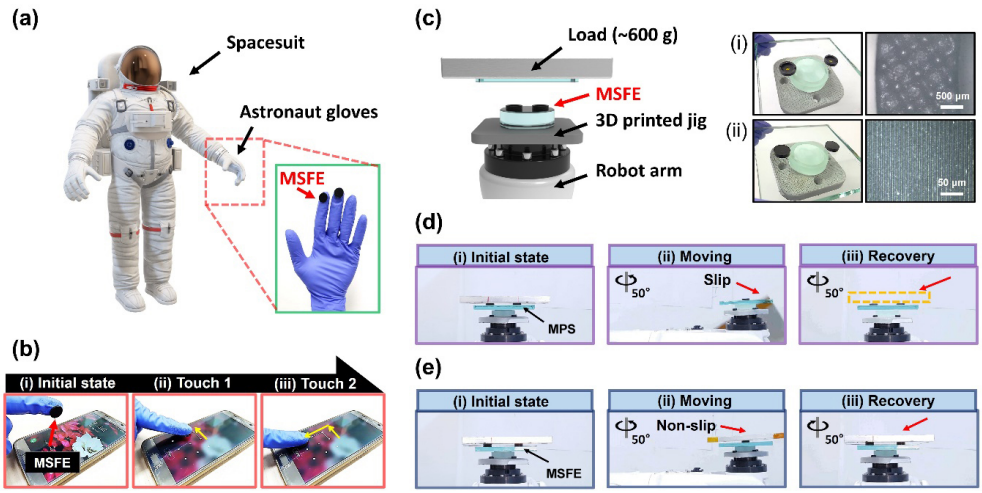

Fig. 5 (a) Schematic of the MSFE applied in astronaut gloves as the 1st application. The MSFE was attached onto the end of the gloves. (b) Time-lapse images for the conductivity test of MSFE. The electric signal could be transmitted through the MSFE: (i) initial state, (ii) screen touching, and (iii) continuously touch. (c) Schematic of the MSFE applied in glass transfer systems as the 2nd application. The MSFE was assembled with the 6-DOF robot arm: (i) photograph and microscope images of the MPS; and (ii) photograph and microscope images of the MSFE. (d) Time-lapse images for the MPS-applied glass transfer system. (e) Time-lapse images for the MSFE-applied glass transfer system. The time period from the initial state to the recovery in the images is around 10–15 seconds.

The MSFE and MPS were assembled on the robot arm by using a 3D printed jig. As shown in Figs. 5(d) and 5(e), a glass attached jig (600 g) was placed on the MPS and MSFE as a load, and the robot arm was operated with a rotation radius of 280 mm, a high rotation speed of 480 (°)·s^{-1}, and a rotation angle of 50°. In the case of the MPS (Fig. 5(d)), the jig was escaped by the centrifugal force and the inertia due to low friction, meanwhile, in the case of the MSFE (Fig. 5(e)), non-slip occurred due to high frictional force, and it could be stably returned to the initial state without any issue (Movies S1 and S2 in the ESM). This experiment showed the advanced and enhanced frictional force of the MSFE compared with the MPS, which has been used in real glass transfer systems. This experiment revealed that the MSFE could be utilized efficiently for advanced glass transfer systems.

4 Conclusions

In this study, we report an MSFE that not only have high frictional force but also electric conductivity inspired by the role of fingerprint.

In summary, the main conclusions are as follows:

1) Fingerprint-inspired advanced end-effector was developed with a fluorocarbon rubber. So far, the fabrication of microstructured samples composed with the fluorocarbon rubber has been limited. In this study, we developed a new fabrication method using the thin PDMS mold. Based on the main role of fingerprint, the MSFE was designed with high friction and conductivity.

2) The MSFE exhibits admirable friction with a value of ~22.3 N which is a higher value up to 4.5 times compared with the frictional force of MPS. This is a noticeable achievement in the development of end-effector, and the role of microstructures on the MSFE was analyzed in detail from the mechanical engineering perspective view.

3) Due to the material characteristic of the fluorocarbon rubber, the MSFE is not only durable but also usable in harsh conditions such as a high temperature and vacuum environment. We verified the reliability of the MSFE through the repeat test up to 100,000 cycle and the TGA test.

4) Based on various experiments, we suggest specific and practical applications of the MSFE. The glass transfer systems and astronaut gloves with MSFE were introduced. We observed the biosignal transmission and enhancement of the friction via an astronaut glove and a glass transfer robot system. Despite a high rotation speed of robot arm (480 (°)·s^{-1}), the jig on the MSFE was stably placed against the centrifugal force, whereas in case of the MPS, the jig was escaped. Through this experiment, we confirmed the strong chance to apply the MSFE to real industrial fields.

Lastly, we emphasize that the MSFE could become one of the breakthroughs in the demand for advanced non-slip pads for the next-generation glass transfer systems, and the MSFE is expected to be applied in various fields, such as the next-generation glass transfer systems and astronaut gloves.

Acknowledgements

This work was supported by the National Research Foundation of Korea Grant (NRF-2020R1A4A1018652 and 2019R1A2C1086766) and Bridge program by the Korea Environmental Industry & Technology Institute (2021002800015), which was funded by the Korean government.

Electronic Supplementary Material Supplementary material is available in the online version of this article at https://doi.org/10.1007/s40544-022-0612-y.

References

[1] Egan P, Sinko R, LeDuc P R, Keten S. The role of mechanics in biological and bio-inspired systems. *Nat Commun* **6**: 7418 (2015)

[2] Brady R M. Optimization strategies gleaned from biological evolution. *Nature* **317**(6040): 804–806 (1985)

[3] Hill B. Living nature as a source of ideas for new product solutions. In: Proceedings of the International Scientific and Practical Conference, 2007: 36–45.

[4] Chen Y P, Meng J X, Gu Z, Wan X Z, Jiang L, Wang S T. Bioinspired multiscale wet adhesive surfaces: Structures and controlled adhesion. *Adv Funct Mater* **30**(5): 1905287 (2020)

[5] Gao Z L, Lin G L, Chen Y C, Zheng Y P, Sang N, Li Y F, Chen L, Li M C. Moth-eye nanostructure PDMS films for reducing reflection and retaining flexibility in ultra-thin c-Si solar cells. *Sol Energy* **205**: 275–281 (2020)

[6] Chen Q, Hubbard G, Shields P A, Liu C, Allsopp D W E, Wang W N, Abbott S. Broadband moth-eye antireflection coatings fabricated by low-cost nanoimprinting. *Appl Phys Lett* **94**(26): 263118 (2009)

[7] Liu Y, Chen B D, Li W, Zu L L, Tang W, Wang Z L. Bioinspired triboelectric soft robot driven by mechanical energy. *Adv Funct Mater* **31**(38): 2104770 (2021)

[8] Glick P, Suresh S A, Ruffatto D, Cutkosky M, Tolley M T, Parness A. A soft robotic gripper with gecko-inspired adhesive. *IEEE Robotics Autom Lett* **3**(2): 903–910 (2018)

[9] Wang S H, Luo H Y, Linghu C H, Song J Z. Elastic energy storage enabled magnetically actuated, octopus-inspired smart adhesive. *Adv Funct Mater* **31**(9): 2009217 (2021)

[10] Fu S C, Zhong X L, Zhang Y, Lai T W, Chan K C, Lee K Y, Chao C Y H. Bio-inspired cooling technologies and the applications in buildings. *Energy Build* **225**: 110313 (2020)

[11] Yi H, Lee S H, Seong M, Kwak M K, Jeong H E. Bioinspired reversible hydrogel adhesives for wet and underwater surfaces. *J Mater Chem B* **6**(48): 8064–8070 (2018)

[12] Baik S Y, Kim D W, Park Y J, Lee T J, Bhang S H, Pang C H. A wet-tolerant adhesive patch inspired by protuberances in suction cups of octopi. *Nature* **546**(7658): 396–400 (2017)

[13] Sha X Y, Zhang C X, Qi M W, Zheng L H, Cai B K, Chen F, Wang Y L, Zhou Y F. Mussel-inspired alternating copolymer as a high-performance adhesive material both at dry and under-seawater conditions. *Macromol Rapid Commun* **41**(10): 2000055 (2020)

[14] Wang S, Fang Y L, He H, Zhang L, Li C A, Ouyang J Y. Wearable stretchable dry and self-adhesive strain sensors with conformal contact to skin for high-quality motion monitoring. *Adv Funct Mater* **31**(5): 2007495 (2021)

[15] Lin C H, Huang C Y, Ho J Y, Hsueh H Y. Symmetrical wrinkles in single-component elastomers with fingerprint-inspired robust isotropic dry adhesive capabilities. *ACS Appl Mater Interfaces* **12**(19): 22365–22377 (2020)

[16] Lee S H, Hwang I, Kang B S, Jeong H E, Kwak M K. Highly flexible and self-adaptive dry adhesive end-effectors for precision robotics. *Soft Matter* **15**(29): 5827–5834 (2019)

[17] Liang R L, Hu R, Long H L, Huang X Y, Dai J N, Xu L L, Ye L, Zhai T Y, Kuo H C, Chen C Q. Bio-inspired flexible fluoropolymer film for all-mode light extraction enhancement. *ACS Appl Mater Interfaces* **11**(21): 19623–19630 (2019)

[18] Zhang Z X, Wang L, Yu H T, Zhang F, Tang L, Feng Y Y, Feng W. Highly transparent, self-healable, and adhesive organogels for bio-inspired intelligent ionic skins. *ACS Appl Mater Interfaces* **12**(13): 15657–15666 (2020)

[19] Purtov J, Frensemeier M, Kroner E. Switchable adhesion in vacuum using bio-inspired dry adhesives. *ACS Appl Mater Interfaces* **7**(43): 24127–24135 (2015)

[20] Wang Z, Ding H L, Liu D L, Xu C H, Li B, Niu S C, Li J, Liu L P, Zhao J, Zhang J Q, et al. Large-scale bio-inspired flexible antireflective film with scale-insensitivity arrays. *ACS Appl Mater Interfaces* **13**(19): 23103–23112 (2021)

[21] Shahsavan H, Salili S M, Jákli A, Zhao B X. Thermally active liquid crystal network gripper mimicking the self-peeling of gecko toe pads. *Adv Mater* **29**(3): 1604021 (2017)

[22] Dass S C. Fingerprint-based recognition. *Int Stat Rev* **81**(2): 175–187 (2013)

[23] Haraksim R, Galbally J, Beslay L. Fingerprint growth model for mitigating the ageing effect on children's fingerprints matching. *Pattern Recognit* **88**: 614–628 (2019)

[24] Hong L, Wan Y F, Jain A. Fingerprint image enhancement: Algorithm and performance evaluation. *IEEE Trans Pattern Anal Mach Intell* **20**(8): 777–789 (1998)

[25] Jain A, Hong L, Bolle R. On-line fingerprint verification. *IEEE Trans Pattern Anal Mach Intell* **19**(4): 302–314 (1997)

[26] Karu K, Jain A K. Fingerprint classification. *Pattern Recognit* **29**(3): 389–404 (1996)

[27] Dahiya R S, Gori M. Probing with and into fingerprints. *J Neurophysiol* **104**(1): 1–3 (2010)

[28] Prevost A, Scheibert J, Debrégeas G. Effect of fingerprints orientation on skin vibrations during tactile exploration of textured surfaces. *Commun Integr Biol* **2**(5): 422–424 (2009)

[29] Scheibert J, Leurent S, Prevost A, Debrégeas G. The role of fingerprints in the coding of tactile information probed with a biomimetic sensor. *Science* **323**(5920): 1503–1506 (2009)

[30] Lee S H, Kim H S, Song H W, Kwak M K. Fluorocarbon rubber-based inert dry adhesive for applications under harsh conditions. *ACS Appl Polym Mater* **3**(8): 3981–3988 (2021)

[31] Banik I, Bhowmick A K, Raghavan S V, Majali A B, Tikku V K. Thermal degradation studies of electron beam cured terpolymeric fluorocarbon rubber. *Polym Degrad Stab* **63**(3): 413–421 (1999)

[32] Yeo Y G, Park H H, Lee C S. A study on the characteristics of a rubber blend of fluorocarbon rubber and hydrogenated nitrile rubber. *J Ind Eng Chem* **19**(5): 1540–1548 (2013)

[33] Pham T T, Sridhar V, Kim J K. Fluoroelastomer–MWNT nanocomposites-1: Dispersion, morphology, physico-mechanical, and thermal properties. *Polym Compos* **30**(2): 121–130 (2009)

[34] Peacock R N. Practical selection of elastomer materials for vacuum seals. *J Vac Sci Technol* **17**(1): 330–336 (1980)

[35] Shajari S. Development of multifunctional polymer nano-composites with hybrid structures for fabrication of stretchable strain sensing and wearable electronic devices. Ph.D. Thesis. Calgary (Canada): University of Calgary, 2020.

[36] Ryu H J, Hang N T, Lee J H, Choi J Y, Choi G, Choy J H. Effect of organo-smectite clays on the mechanical properties and thermal stability of EVA nanocomposites. *Appl Clay Sci* **196**: 105750 (2020)

[37] Lee I S, Kim J G. Industrial demand and integrated material flow of terbium in Korea. *Int J Precis Eng Manuf Green Technol* **1**(2): 145–152 (2014)

[38] Kang O H, Lee S H, Yun J H, Yi H, Kwak M K, Lee S R. Adhesion tunable bio-inspired dry adhesives by twisting. *Int J Precis Eng Manuf* **18**(10): 1433–1437 (2017)

[39] Li Y S, Krahn J, Menon C. Bioinspired dry adhesive materials and their application in robotics: A review. *J Bionic Eng* **13**(2): 181–199 (2016)

[40] Lee S H, Kim H S, Song H W, Kwak M K. Fluorocarbon rubber-based inert dry adhesive for applications under harsh conditions. *ACS Appl Polym Mater* **3**(8): 3981–3988 (2021)

[41] Jiang H, Hawkes E W, Fuller C, Estrada M A, Suresh S A, Abcouwer N, Han A K, Wang S Q, Ploch C J, Parness A, et al. A robotic device using gecko-inspired adhesives can grasp and manipulate large objects in microgravity. *Sci Robot* **2**(7): eaan4545 (2017)

[42] Hu Q Q, Dong E B, Sun D. Soft gripper design based on the integration of flat dry adhesive, soft actuator, and microspine. *IEEE Trans Robotics* **37**(4): 1065–1080 (2021)

[43] Lee S H, Kim S W, Kang B S, Chang P S, Kwak M K. Scalable and continuous fabrication of bio-inspired dry adhesives with a thermosetting polymer. *Soft Matter* **14**(14): 2586–2593 (2018)

[44] Choi S J, Kim H N, Bae W G, Suh K Y. Modulus- and surface energy-tunable ultraviolet-curable polyurethane acrylate: Properties and applications. *J Mater Chem* **21**(38): 14325–14335 (2011)

[45] Bae W G, Kim H N, Kim D, Park S H, Jeong H E, Suh K Y. 25th anniversary article: Scalable multiscale patterned structures inspired by nature: The role of hierarchy. *Adv Mater* **26**(5): 675–700 (2014)

[46] Chou S Y. Nanoimprint lithography. *J Vac Sci Technol B* **14**(6): 4129 (1996)

[47] Guo L J. Nanoimprint lithography: Methods and material requirements. *Adv Mater* **19**(4): 495–513 (2007)

[48] Corning D. Information about high technology silicone materials, available from Dow Corning Corp. (1991).

[49] Whitesides G M. The origins and the future of microfluidics. *Nature* **442**(7101): 368–373 (2006)

[50] Packham D E. Work of adhesion: Contact angles and contact mechanics. *Int J Adhesion Adhesives* **16**(2): 121–128 (1996)

[51] Rogers J A, Lee H H. *Unconventional Nanopatterning Techniques and Applications*. Hoboken (USA): Wiley, 2008: 7–8.

[52] Ma P C, Liu M Y, Zhang H, Wang S Q, Wang R, Wang K, Wong Y K, Tang B Z, Hong S H, Paik K W, et al. Enhanced electrical conductivity of nanocomposites containing hybrid fillers of carbon nanotubes and carbon black. *ACS Appl Mater Interfaces* **1**(5): 1090–1096 (2009)

[53] Medalia A I. Electrical conduction in carbon black composites. *Rubber Chem Technol* **59**(3): 432–454 (1986)

[54] Sumita M, Sakata K, Asai S, Miyasaka K, Nakagawa H. Dispersion of fillers and the electrical conductivity of polymer blends filled with carbon black. *Polym Bull* **25**(2): 265–271 (1991)

[55] Gere J M, Timoshenko S P. *Mechanics of Materials,* 5th edn. Pacific Grove (USA): Springer US, 2001.

[56] Johnson K L, Kendall K, Roberts A D. Surface energy and the contact of elastic solids. *Proc R Soc A* **324**(1558): 301–313 (1971)

[57] Marshall J S, Li S Q. *Adhesive Particle Flow*. Cambridge (UK): Cambridge University Press, 2014.

[58] Kamperman M, Kroner E, del Campo A, McMeeking R M, Arzt E. Functional adhesive surfaces with “gecko” effect: The concept of contact splitting. *Adv Eng Mater* **12**(5): 335–348 (2010)

[59] Arzt E, Gorb S, Spolenak R. From micro to nano contacts in biological attachment devices. *Proc Natl Acad Sci* **100**(19): 10603–10606 (2003)

Sung Ho LEE. He received his Ph.D. degree in mechanical engineering in 2020 from Kyungpook National University, Republic of Korea. He is now a research fellow at the Department of Electrical Engineering and Computer Science of the University of Michigan, USA. His research interests are bio-compatible adhesive, soft robotics, optical sensors, etc.

Hyo Sung KIM. He received his M.S. degree in mechanical engineering in 2000 from Kyungpook National University, Republic of Korea. He is now a Ph.D. candidate at Kyungpook National University, Republic of Korea. His research interest is friction-enhanced surface with fluorocarbon rubber.

Han Jun PARK. He received his B.S. degree in mechanical engineering in 2021 from Kyungpook National University, Republic of Korea. He is now a student of M.S. degree course at Kyungpook National University. His research interests are soft robotics and dry adhesive inspired by the gecko foot.

Moon Kyu KWAK. He received his Ph.D. degree in mechanical and aerospace Engineering in 2011 from Seoul National University, Republic of Korea. He is now a professor at the Department of Mechanical Engineering of Kyungpook National University, Republic of Korea. His research interests are functional surfaces based on the micro/nano structures such as friction-enhanced surfaces, dry adhesive, R2R systems, and so on.